Electronic Supplementary Information (**ESI**):

Peroxynitrite Chemistry Derived from Nitric Oxide Reaction with a Cu(II)-OOH Species and a new Copper Mediated NO Reductive Coupling Reaction

Sunghee Kim, Maxime A. Siegler, and Kenneth D. Karlin
Department of Chemistry, Johns Hopkins University, Baltimore, Maryland 21218

Contents:

1. Materials and methods.

General. All materials used were commercially available analytical grade from Sigma-Aldrich chemicals and TCI. Acetone was distilled under an inert atmosphere over $CaSO_4$ and degassed under argon prior to use. Diethyl ether was used after being passed through a 60 cm long column of activated alumina (Innovative Technologies) under argon. Tetrahydrofuran (THF) was distilled under an inert atmosphere from Na/benzophenone and degassed with argon prior to use. Pentane was freshly distilled from calcium hydride under an inert atmosphere and degassed prior to use. $[Cu^I(CH_3CN)_4]BArF$ ($BArF = B(C_6F_5)_4$) were synthesized according to literature protocols, and their identity and purity were verified by elemental analysis and/or ^{1}H-NMR.[a,b] Synthesis and manipulations of copper salts were performed according to standard Schlenk techniques or in an MBraun glovebox (with O_2 and H_2O levels below 1 ppm). Nitrous oxide (N_2O) gas was purchased from Airgas as a custom mixture, at a concentration of 250 ppm, balanced with dinitrogen at 1 atm. Deoxygenation of solvents was effected by either repeated freeze/pump/thaw cycles or bubbling with argon for 30 - 45 minutes.

[a] Liang, H. C. et al., *Inorg. Chem.* **2002**, *41,* 2209-2212.

[b] Caughey, W. S. et al., *J. Org. Chem*. **1966**, *31*, 1978-1982.

Instrumentation. UV-Vis spectra were recorded with an HP Model 8453A diode array spectrophotometer equipped with a liquid nitrogen chilled Unisoku USP-203-A cryostat. NMR spectroscopy was performed on Bruker 300 and 400 MHz instruments with spectra calibrated to either internal tetramethylsilane (TMS) standard or to residual protio solvent. EPR measurements were performed on an X-Band Bruker EMX CW EPR controlled with a Bruker ER 041 XG microwave bridge operating at the X-band (~9 GHz). Gas chromatography (GC) was performed on an Agilent 6890 gas chromatograph fitted with a HP-5 (5%-phenyl)-methylpolysiloxane capillary column (30 m * 0.32 mm* 0.25 mm) and equipped with a flame-ionization detector. The GC-FID response factors for benzaldehydes were prepared *vs.* dodecane as an internal standard. ESI Mass spectra were acquired using a Finnigan LCQDeca ion-trap mass spectrometer equipped with an electrospray ionization source (Thermo Finnigan, San Jose, CA). GC-Mass experiments were carried out and recorded using a Shimadzu GC-17A/GCMS0QP5050 gas chromatograph/mass spectrometer. X-ray diffraction was performed at the X-ray diffraction facility at the Johns Hopkins University. The X-ray intensity data were measured on an Oxford Diffraction Xcalibur3 system equipped with a graphite monochromator and an Enhance (Mo) X-ray Source (λ = 0.71073Å) operated at 2 kW power (50 kV, 40 mA) and a CCD detector. The frames were integrated with the Oxford Diffraction *CrysAlisRED* software package. Gas chromatography (GC) headspace analysis was performed on a Varian CP-3800 instrument equipped with ECD detection and a Restek ShinCarbon ST 80/100 molecular sieve packed column.

2. •$NO_{(g)}$ purification.

Nitrogen monoxide (•NO) gas was obtained from Matheson Gases and purified as follows (Figure S1): It was first passed through multiple columns containing Ascarite II (NaOH on non- fibrous silicate carrier, purchased from Thomas Scientific) to remove higher nitrogen oxide impurities. Further purification by distillation was completed by warming frozen •$NO_{(g)}$ (as crystalline N_2O_2) from 78 K in a liquid N_2 cooled trap to 193 K through use of an acetone/dry-ice (–80 ^{o}C) bath, and collection in a second liquid N_2 cooled evacuated Schlenk flask. This secondary flask was again warmed to 193 K and the purified •$NO_{(g)}$ was collected in an evacuated Schlenk flask (typically 50 mL) fitted with a septum. The •$NO_{(g)}$ in the Schlenk flask is collected and kept at higher pressures (> 1 atm, septum bulges outward due to high pressures inside the Schlenk flask). Addition of •$NO_{(g)}$ to metal complex solutions was effected by transfer *via* a three-way long syringe needle connected to a Schlenk line.

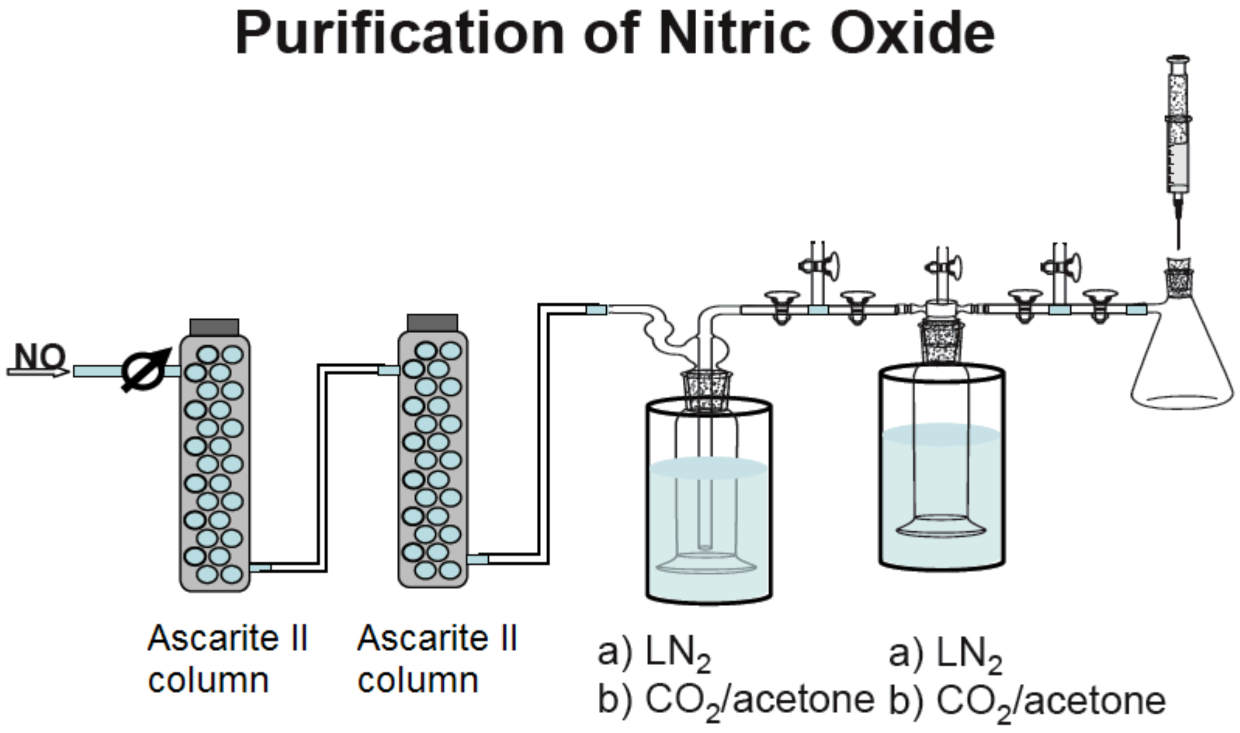

Figure S1. Scheme representing the purification setup for •$NO_{(g)}$.

3. Synthesis of Cu(I) and Cu(II) complexes.

Procedures for synthesizing $[(BA)Cu^{II}(CH_3COCH_3)](ClO_4)_2$ (**1**) and $[(BA)Cu^{I}]$BArF have been previously described.[c]

$[(BA)Cu^{II}(CH_3COCH_3)](ClO_4)_2$ (**1**) complex. **Elemental analysis:** ($C_{25}H_{27}Cl_2CuN_5O_9$) Calculated: C (44.42), H (4.03), N (10.36); found: C (44.48), H (4.77), N (10.18). **EPR spectrum**: X-band (ν = 9.186 GHz) spectrometer in acetone at 70 K: $g_{||}$ = 2.07, $A_{\perp}$ = 108 G, $g_{\perp}$ = 2.22.

$[(BA)Cu^{I}]B(C_6F_5)_4$ complex. **^{1}H-NMR** (400 MHz, acetone-d_6): δ 8.4 (s, 3H), 7.75 (s, 2H), 7.6-7.30 (m, 11H), 5.02 (s, 4H, $2CH_2Ph$), 3.76 (m, 2H, CH_2Py), 1.92 (t, 2H, CH_2Ph). **Elemental analysis:** ($C_{49}H_{25}BCuF_{20}N_5$) Calculated: C (51.71), H (2.21), N (6.15); found: C (51.18), H (2.18), N (5.65).

[c] S. Kim, C. Saracini, M. A. Siegler, N. Drichko and K. D. Karlin, *Inorg. Chem.*, 2012, **51**, 12603.

4. Generation of [(BA)Cu^{II}-OOH]$^+$ (2)

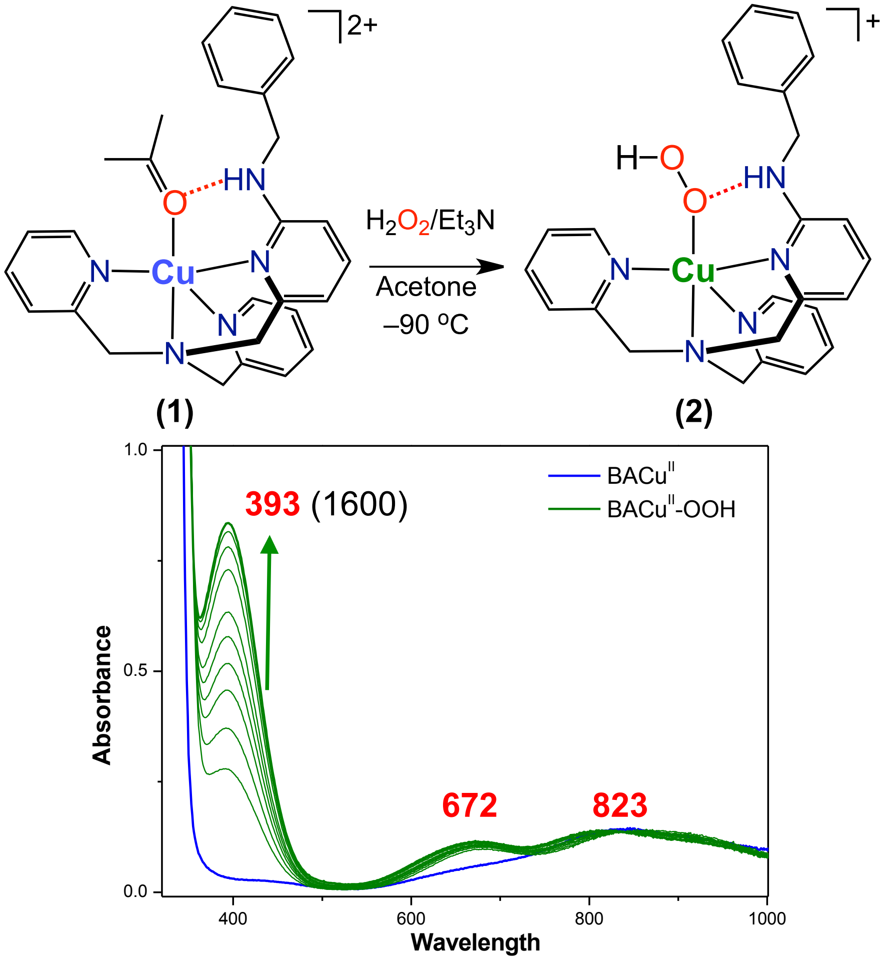

Figure S2. [(BA)Cu^{II}-OOH]$^+$ (**2**) was generated at −90 °C in acetone under Ar by reacting complex **1** with one equiv H_2O_2/Et_3N prepared by repeated freeze/pump/thaw cycles under Ar. Also shown are UV-Vis spectra illustrating the formation of **2** (0.6 mM) at 393 (ε = 1,600 $M^{-1}cm^{-1}$), 672 (ε = 260 $M^{-1}cm^{-1}$) and 823 (ε = 310 $M^{-1}cm^{-1}$) nm.

5. ESI-MS spectrum of $[(BA)Cu^{II}(NO_3)]^+$ (3)

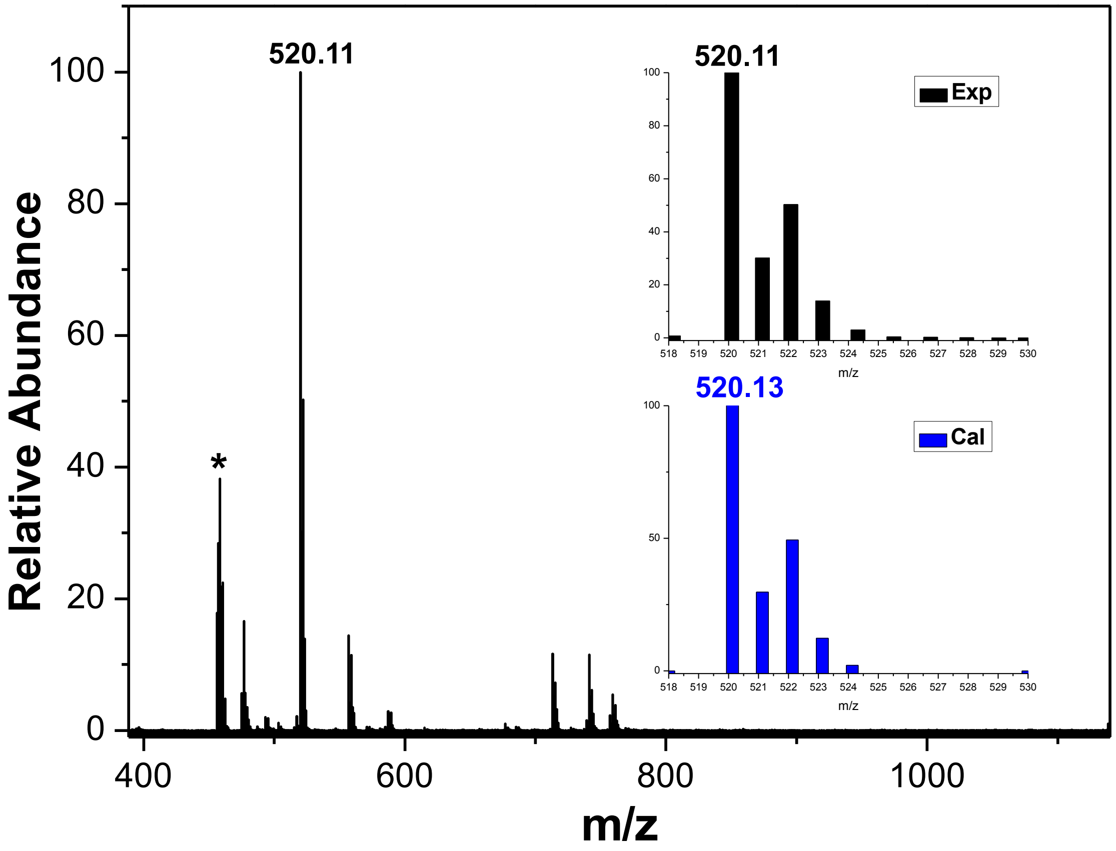

Figure S3. ESI-MS spectrum of the $[(BA)Cu^{II}(NO_3^-)]^+$ (**3**) from the reaction of $[(BA)Cu^{II}(OOH)]^+$ (**2**) with nitric oxide. The peak at m/z = 458.38 labeled with an asterisk was assigned to $[(BA)Cu^{I}]^+$. Inset: isotope distribution patterns.

6. Generation of $[(BA)Cu^{II}\text{-}NO_3]^+$

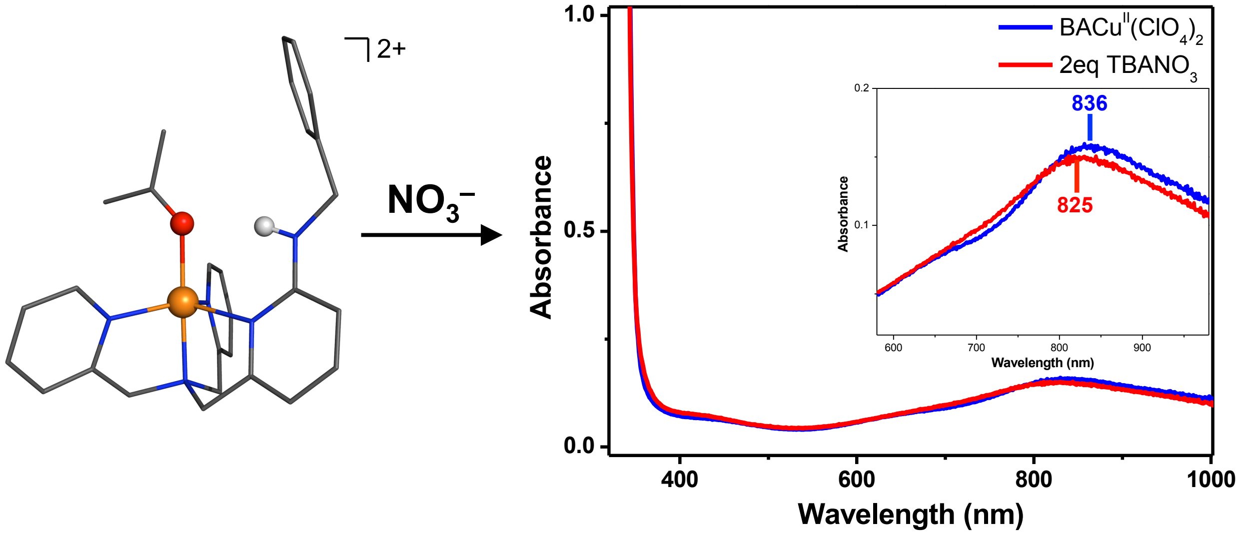

Figure S4. UV-vis spectrum of the reaction of **1** with 2 equiv tetrabutylammonium nitrate ($TBANO_3$) in acetone at -90 °C.

7. Generation of $[(BA)Cu^{II}\text{-}NO_2]^+$

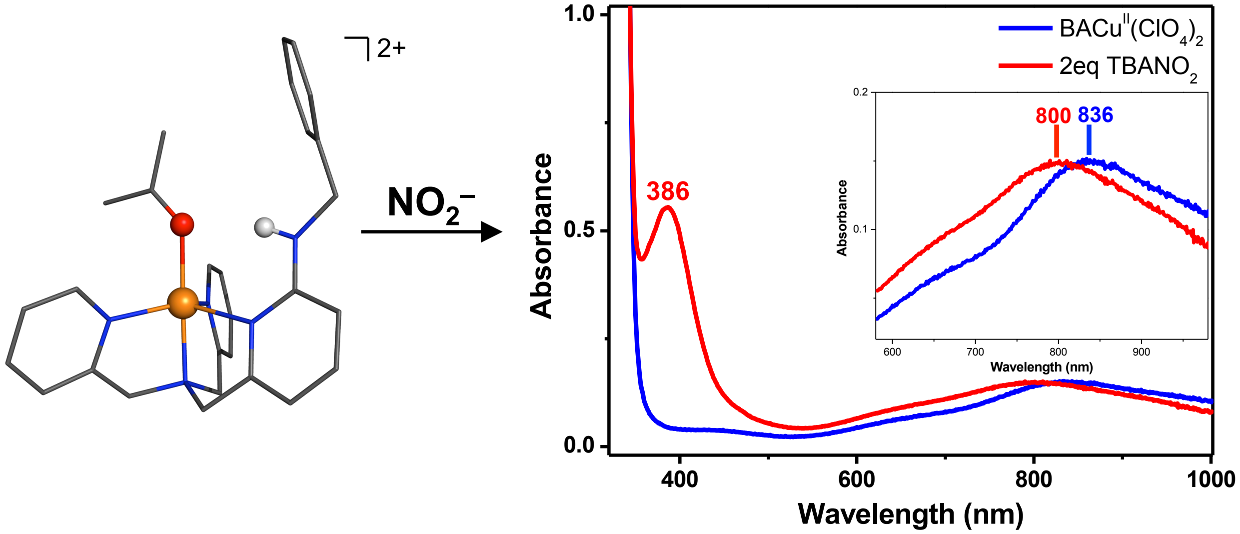

Figure S5. UV-vis spectrum of the reaction of **1** with 2 equiv tetrabutylammonium nitrite, ($TBANO_2$) in acetone at -90 °C. A Cu-NO_2^- complex shows the charge transfer band at 386 nm.

8. EPR data

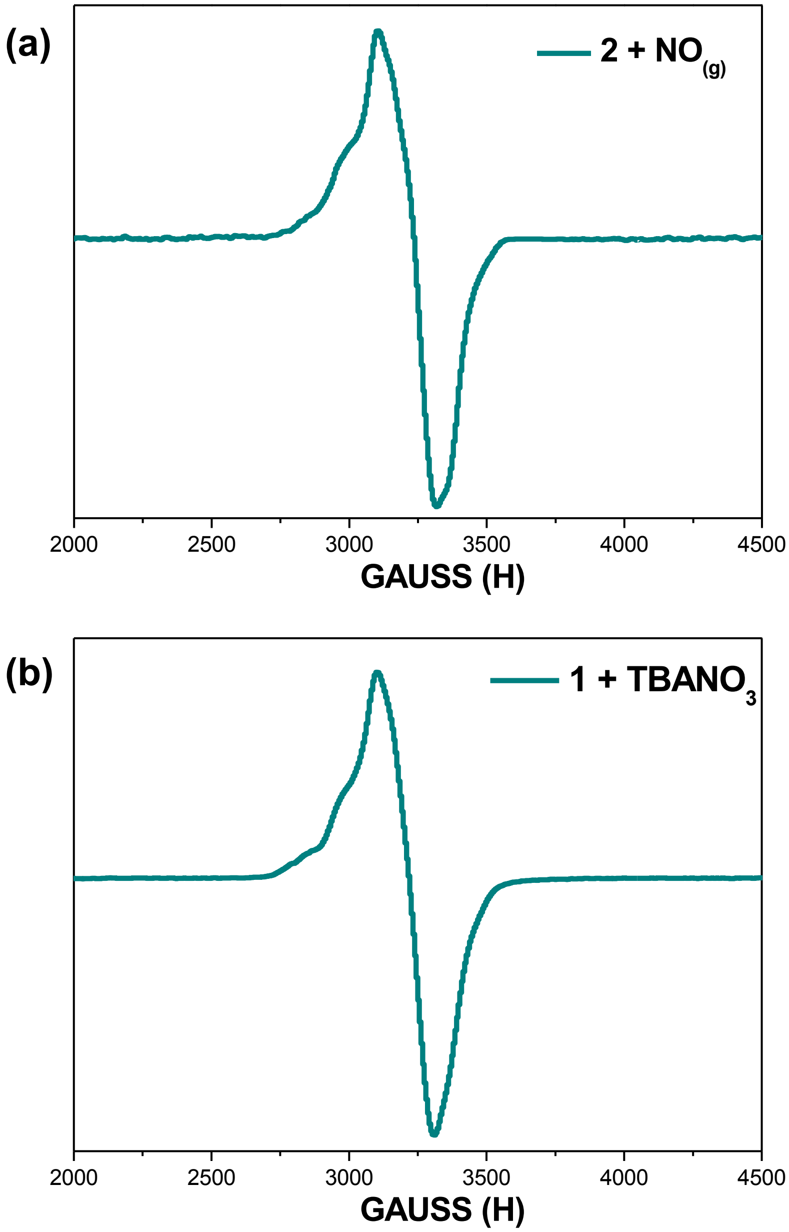

Figure S6. EPR data of the reaction of $[(BA)Cu^{II}\text{-}OOH]^+$, (**2**) (2 mM) with (a) •NO ($g_\perp = 2.10$) and (b) the reaction of $[(BA)Cu^{II}(CH_3COCH_3)](ClO_4)_2$ (**1**) with $TBANO_3$ ($g_\perp = 2.10$) (X-band, $\nu = 9.186$ GHz; acetone at 70 K).

9. X-ray crystallography.

Single crystals were obtained by vapor diffusion of diethyl ether into a solution of the complex in acetone. All reflection intensities were measured at 110(2) K using a KM4/Xcalibur (detector: Sapphire3) with enhance graphite-monochromated Mo $K\alpha$ radiation ($\lambda = 0.71073$ Å) under the program CrysAlisPro (Version 1.171.35.11 Oxford Diffraction Ltd., 2011). The program CrysAlisPro (Version 1.171.35.11, Oxford Diffraction Ltd., 2011) was used to refine the cell dimensions. Data reduction was done using the program CrysAlisPro (Version 1.171.35.11, Oxford Diffraction Ltd., 2011). The structure was solved with the program SHELXS-97 (Sheldrick, 2008) and was refined on F^2 with SHELXL-97 (Sheldrick, 2008). Analytical numeric absorption corrections based on a multifaceted crystal model were applied using CrysAlisPro (Version 1.171.35.11, Oxford Diffraction Ltd., 2011). The temperature of the data collection was controlled using the system Cryojet (manufactured by Oxford Instruments). The H atoms (except when specified) were placed at calculated positions using the instructions AFIX 23 or AFIX 43 with isotropic displacement parameters having values 1.2 times Ueq of the attached C atoms. The coordinates and the isotropic factor of the H atom attached to N5 have been refined freely. The structure is ordered. $[(BA)Cu^{II}(NO_3)](ClO_4)$, Fw = 620.50, small blue-green block, 0.28 × 0.17 × 0.16 mm^3, triclinic, P-1 (no. 2), a = 10.2366(15), b = 11.5506(16), c = 12.0967(12) Å, α = 111.662(12), β = 94.591(10), γ = 98.200(12), V = 1301.9(3) Å^3, Z = 2, D_x = 1.583 g cm^{-3}, μ = 0.999 mm^{-1}, abs. corr. range: 0.832–0.897. 12794 Reflections were measured up to a resolution of $(\sin \theta/\lambda)_{max}$ = 0.59 Å^{-1}. 4585 Reflections were unique (R_{int} = 0.0312), of which 4040 were observed [$I > 2\sigma(I)$]. 365 Parameters were refined using 1 restraint. $R1/wR2$ [$I > 2\sigma(I)$]: 0.0298/0.0782. $R1/wR2$ [all refl.]: 0.0357/0.0804. S = 1.059. Residual electron density found between −0.46 and 0.41 e Å^{-3}.

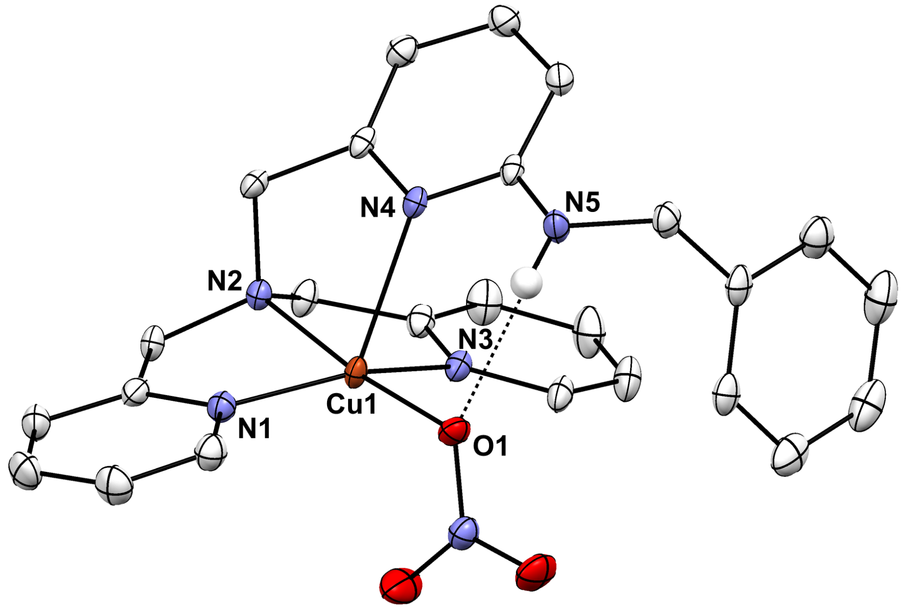

Bond Lengths (Å)

Cu1–N1 = 1.9818(18)
Cu1–N2 = 2.0365(17)
Cu1–N3 = 1.9977(18)
Cu1–N4 = 2.3344(18)
Cu1–O1 = 1.9652(14)

Bond Angles (°)

N1–Cu1–N2 = 82.82(7)
N1–Cu1–N3 = 156.35(7)
N1–Cu1–N4 = 113.18(7)
N1–Cu1–O1 = 99.02(7)
N2–Cu1–N3 = 84.12(7)

N2–Cu1–N4 = 82.62(7)
N2–Cu1–O1 = 173.46(6)
N3–Cu1–N4 = 84.47(7)
N3–Cu1–O1 = 96.18(7)
N4–Cu1–O1 = 90.90(6)

Figure S7. Displacement ellipsoid plot (50 % probability level) of the cationic complex, $[(BA)Cu^{II}(NO_3)]^+$ (**3**). The perchlorate counterion and the H atoms (except for that attached to N5) were removed for clarity.. **Elemental analysis of 3:** ($C_{25}H_{25}ClCuN_6O_7$) Calculated: C (48.39), H (4.06), N (13.54); found: C (48.71), H (4.15), N (13.68).

10. Comparison of the crystal structures.

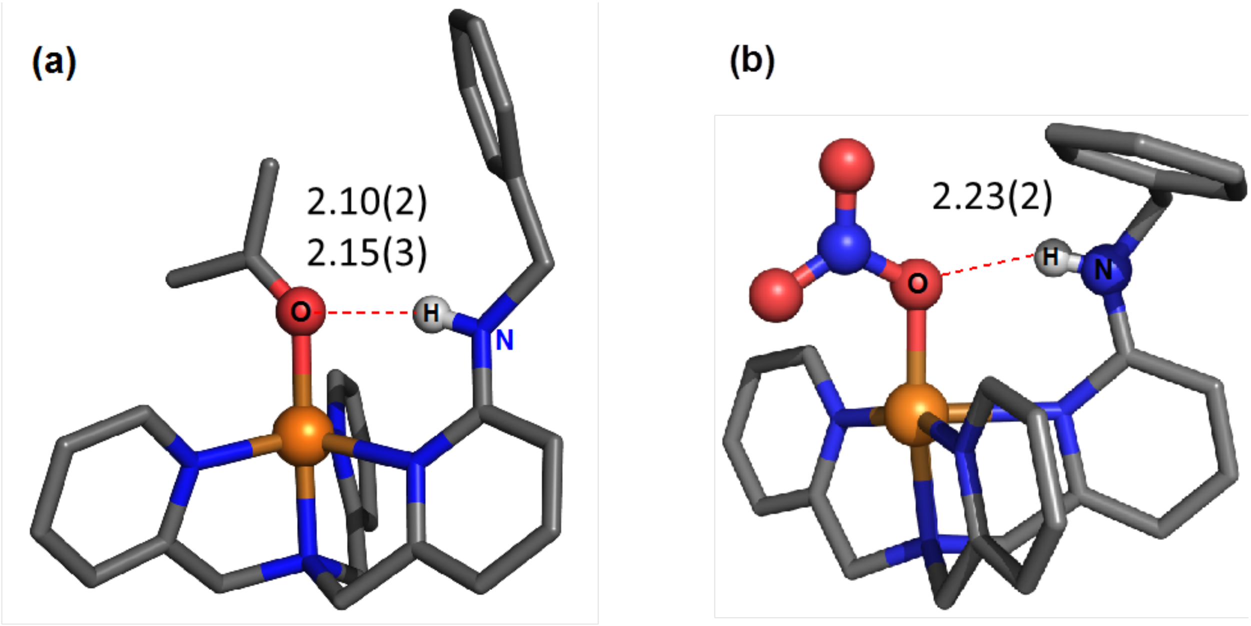

(1)

(3)

Figure S8. (a) The crystal structures of $[(BA)Cu^{II}(CH_3COCH_3)]^{2+}$ (**1**) and $[(BA)Cu^{II}(NO_3^{-})]^{+}$ (**3**) complexes. The two H···O values for (1) are provided as the structure of **1** contains two crystallographically independent unit in the asymmetric unit.

Table S1. Intramolecular N–H…O hydrogen bond interactions found inthe crystal structures of $[BACu^{II}(CH_3COCH_3)]^{2+}$ (**1**) and $[BACu^{II}(NO_3^{-})]^{+}$ (**3**) complexes respectively.

X-ray crystal structures	**H···O (Å)**	**N···O (Å)**	**∠N-H-O**	**τ**
Complex 1, $[(BA)Cu^{II}(CH_3COCH_3)](ClO_4)_2$	**2.10(2)** **2.15(3)**	**2.886(3)** **2.981(3)**	**161(3)** **163(3)**	**0.83**
Complex 3, $[(BA)Cu^{II}(NO_3)](ClO_4)$	**2.23(2)**	**2.963(3)**	**146(2)**	**0.29**

11. Nitration of the 2,4-di-*tert*-butylphenol (2,4-DTBP).

The formation of the Cu-hydroperoxo species (**2**) in acetone at -90 °C was carried out from complex **1** with H_2O_2/Et_3N as described in Figure S2. To this solution, 1 equiv. 2,4-di-*tert*-phenol (2,4-DTBP) was added by syringe from a stock solution of 2,4-DTBP in acetone under Ar. Upon addition of 2,4-DTBP, no UV-vis spectral change was observed. Excess $\bullet NO_{(g)}$ was added into the species **2** using a three-way needle syringe. The solution was stirred at -90 °C for ~10 minutes and then excess $\bullet NO_{(g)}$ was rigorously removed by bubbling the solution with Ar and vacuum purge cycles before warming up to room temperature. A final product was analyzed by injecting the resulting solution directly into a GC instrument. This Product was identified by comparison with an authentic sample, and product yield (~ 80%) of 2,4-di-*tert*-6-nitrophenol was determined by comparison against a standard curve prepared with authentic sample and using dodecane as an internal standard.

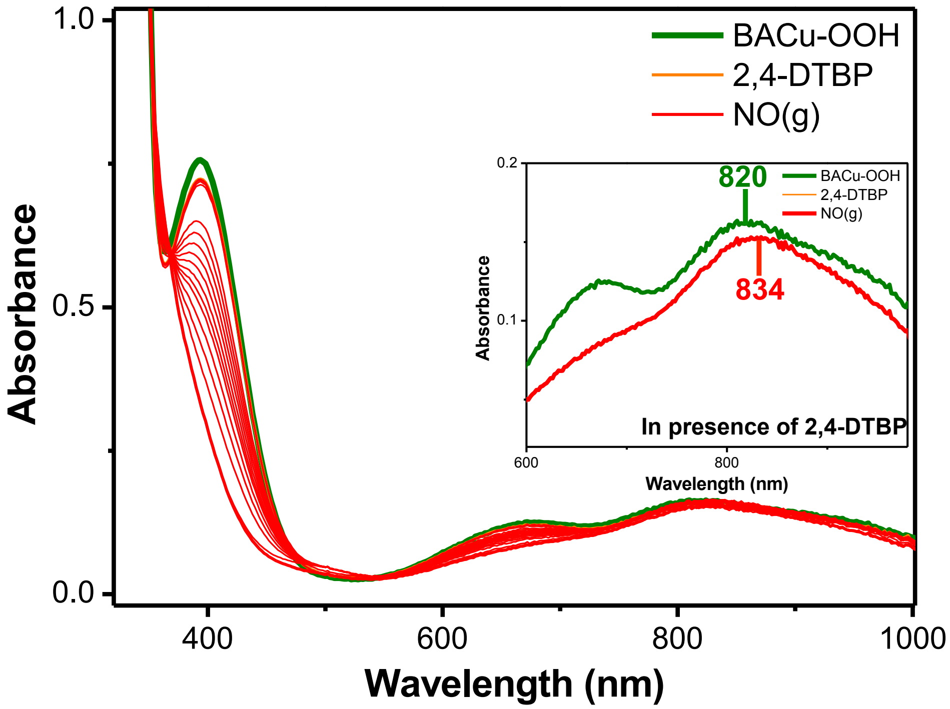

Figure S9. UV-vis spectra of the reaction of (a) $[(BA)Cu^{II}–OOH]^+$(**2**) species in the presence of 2,4-DTBP with $\bullet NO_{(g)}$ giving a nitrated phenol and Cu(II) complex at -90 °C in acetone under Ar.

12. Nitrous oxide quantification by headspace gas chromatography (GC).

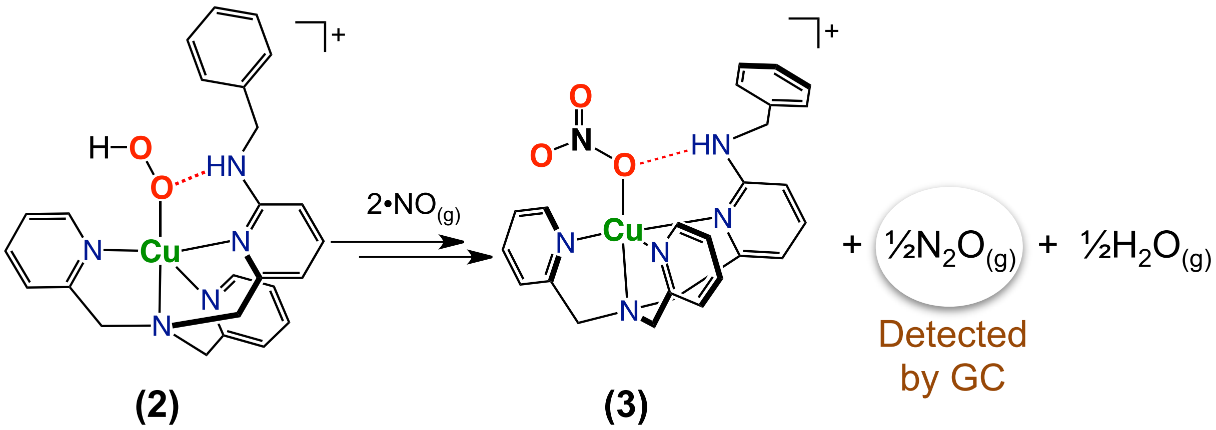

Headspace GC analysis of the above reaction product was performed on a Varian CP-3800 instrument equipped with a 1041 manual injector, electron capture detector, and a packed column (Shincarbon ST 80/100). Grade 5.0 nitrogen was used as both the carrier (8 mL/min) and the make-up (22 mL/min) gas. The injector oven and the detector oven were kept at 200 °C and 300 °C, respectively. All nitrous oxide analyses were performed with the column oven held constant at 150 °C. All gas injections were made using a 60 µL gastight syringe with a sample-lock. 2.5 mL acetone of 1.5 mM solution from the reaction of **2** with $•NO_{(g)}$ was prepared in a modified schlenk cuvette, equipped with a rubber septa under Ar. When the oven temperature is 150 ºC and flow rate equals to 8 mL/min, the retention time is 5.8 min (very sharp peak) for $N_2O_{(g)}$. Nitrogen monoxide gas ($•NO_{(g)}$) possessed a retention time of 2 min (broad leading edge).

13. Controlled experiments.

(a) $Cu^{I} + H^{+} + \bullet NO_{(g)} \rightarrow Cu^{II} + \frac{1}{2}H_2O + \frac{1}{2}N_2O_{(g)}$

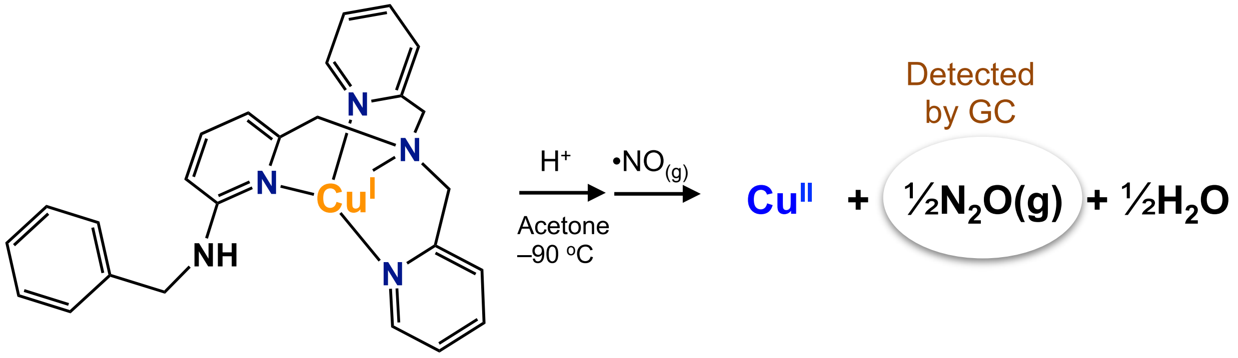

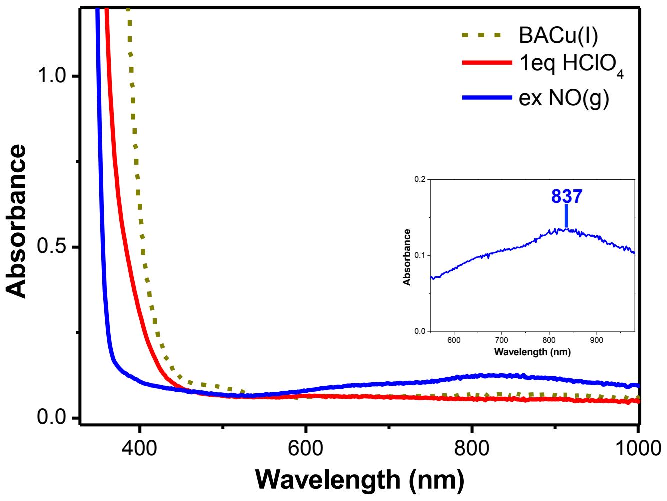

Figure S10. UV-vis spectra of the reaction of $[(BA)Cu^{I}]BArF$ (0.6 mM) + 1 equiv $HClO_4$ with •NO leading to Cu^{II} complex, 0.5equiv $N_2O_{(g)}/H_2O$ at -90 °C in acetone under Ar.

(b) $Cu^I + NO_3^- + H^+ + \bullet NO_{(g)} \rightarrow Cu^{II}\text{-}NO_3^- + \frac{1}{2}N_2O_{(g)} + \frac{1}{2}H_2O$

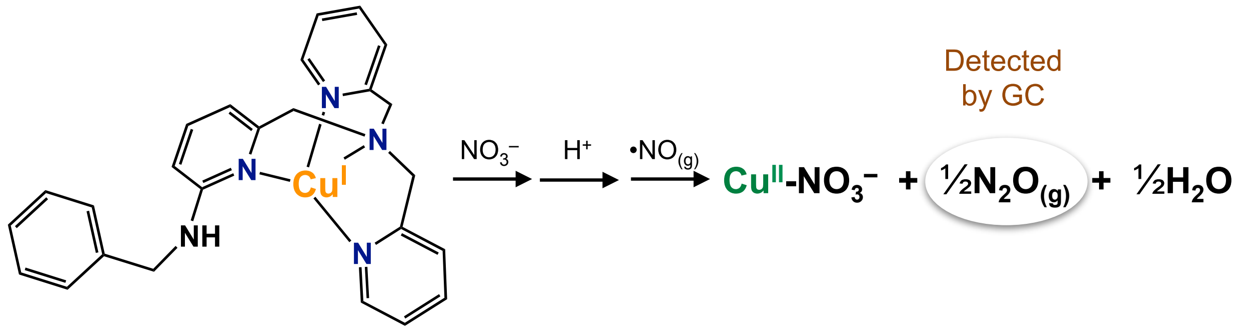

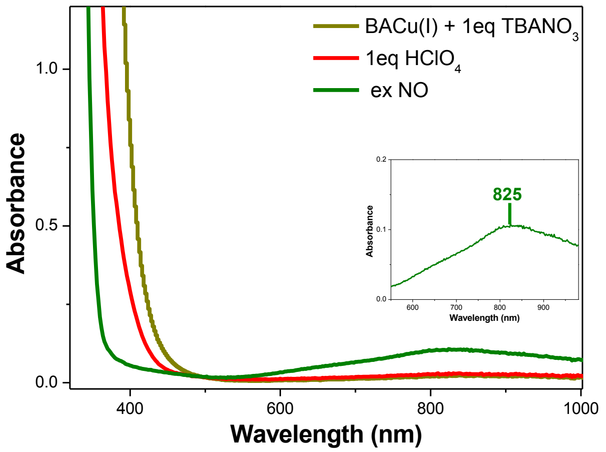

Figure S11. UV-vis spectra of the reaction of (a) [(BA)Cu^I]BArF (0.6 mM)+ 1 equiv TBANO$_3$ + 1 equiv HClO$_4$ with •NO giving $Cu^{II}–NO_3^-$ and 0.5 equiv $N_2O_{(g)}/H_2O$ at -90 °C in acetone under Ar.

(c) $Cu^{I} + 3\bullet NO_{(g)} \rightarrow Cu^{II}\text{- } NO_2^{-} + N_2O_{(g)}$

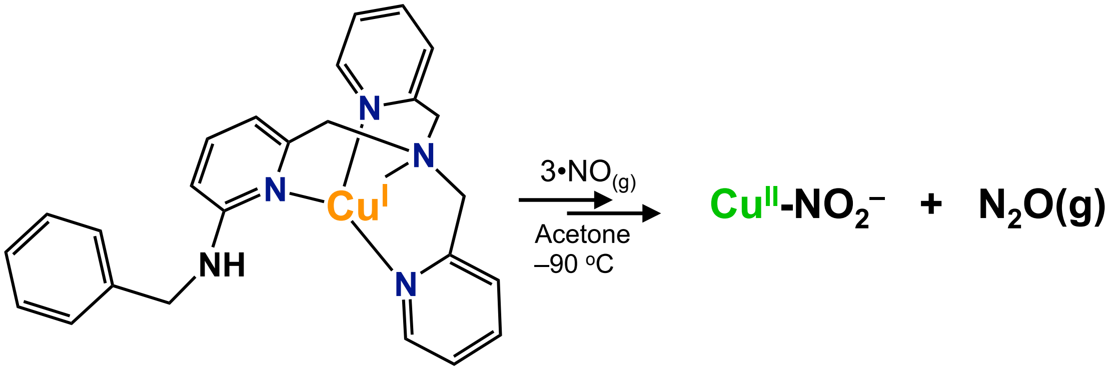

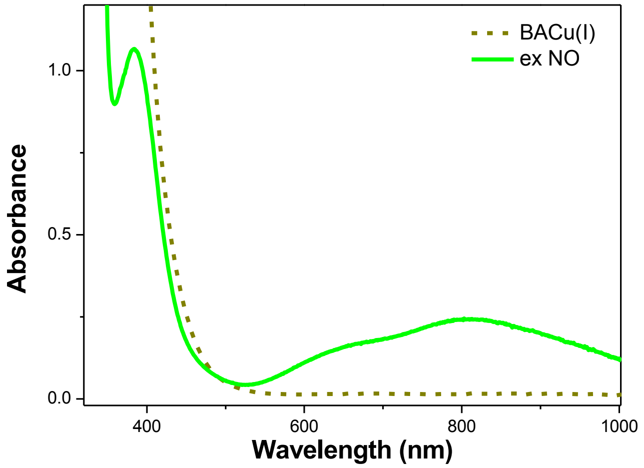

Figure S12. UV-vis spectra of the reaction of (a) $[(BA)Cu^{I}]BArF$ (1 mM) with $3\bullet NO_{(g)}$ at -90 °C in acetone under Ar resulting in $Cu^{II}–NO_2^{-}$ and $N_2O_{(g)}$ which is well known in the literature.

(d) $Cu^{I} + NO_3^{-} + 3•NO_{(g)} \rightarrow Cu^{II}\text{- }NO_2^{-} + N_2O_{(g)} + NO_3^{-}$

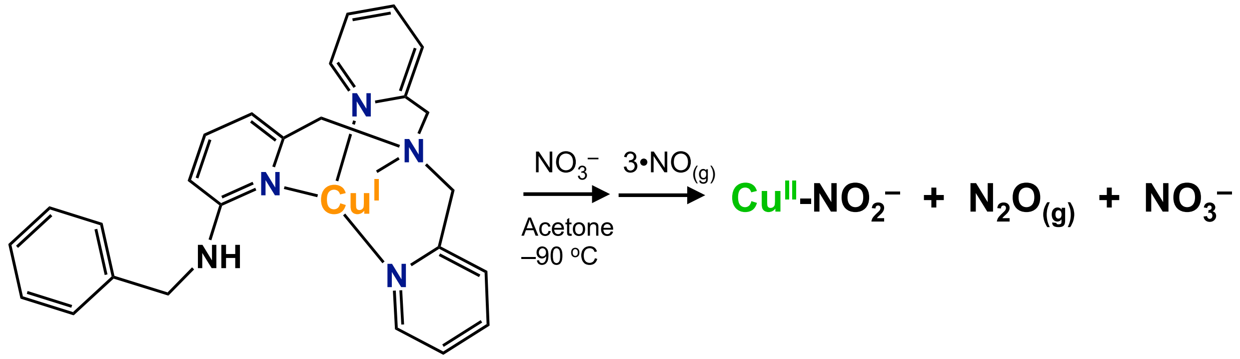

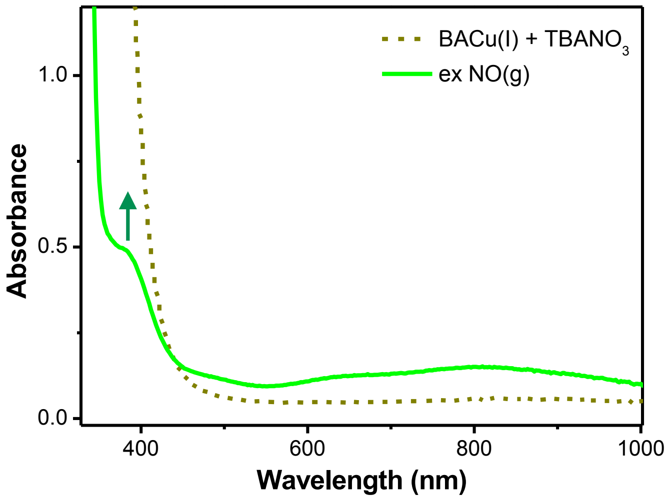

Figure S13. UV-vis spectra of the reaction of (a) $[(BA)Cu^{I}]BArF$ (0.6 mM) with 3•NO in the presence of $TBANO_3$ yielding $Cu^{II}–NO_2^{-}$ and $N_2O_{(g)}$ at -90 °C in acetone under Ar.